Structural classification of the highly disordered crystal phases of [N$_n$][BF$_4$], [N$_n$][PF$_6$], [P$_n$][BF$_4$], and [P$_n$][PF$_6$] salts (N$_n^+$ = tetraalkylammonium and P$_n^+$ = tetraalkylphosphonium)

Kazuhiko Matsumoto,[*,a] Ukyo Harinaga,[a] Ryo Tanaka,[a] Akira Koyama,[a] Rika Hagiwara,[a] and Katsuhiko Tsunashima,[b]

[a]Department of Fundamental Energy Science, Graduate School of Energy Science, Kyoto University

Sakyo-ku, Kyoto 606-8501, Japan

[b]Department of Materials Science, Wakayama National College of Technology, 77 Noshima, Nada-cho, Gobo 644-0023, Japan

* E-mail: k-matsumoto@energy.kyoto-u.ac.jp

S-1. The CsCl'-type structure under the non-centrosymmetric space groups

The structure of the highest temperature soild phase of $[N_1][PF_6]$ was classified into the CsCl'-type under the centrosymmetric group *Im*-3*m*. The other two possible non-centrosymmetric space groups, *I*432 and *I*-43*m*, also give the similar structural type based on the following discussion.

In the case of *I*432, the same discussion with the case of *Im*-3*m* can be applied and the basic ion configuration under *I*432 is identical to that under *Im*-3*m*. The difference between the two space groups is the site symmetry of each site, which affects the orientation of the ions.

Under *I*-43*m*, one of the ions occupies the 2*a* [(0,0,0) and (1/2, 1/2, 1/2)] and 6*b* [(1/2, 1/2, 0), (1/2, 0, 1/2), (0, 1/2, 1/2), (0, 0, 1/2), (0, 1/2, 0), and (1/2, 0, 0)] sites as in the case of *Im*-3*m*, whereas the other occupies the 8*c* site [(x,x,x), (-x,-x,x), (-x,x,-x), (x,-x,-x) and their (1/2,1/2,1/2) translated positions]. Although *x* in the 8*c* site can deviate from 1/4, it should not be large considering the interaction between the cation and anion.

S-2 Calculations of ionic radii and the radius ratio for the highly disordered phases

Ionic radii in the highly disordered crystal structures (Table 3) were estimated from equations (1)−(4) in the main text. The followings are the details for each ion.

$r(PF_6^-)$

$r(PF_6^-)$ was first obtained as an average of the three values from $K[PF_6]$, $Rb[PF_6]$, and $Cs[PF_6]$ using equation (1):

$r(PF_6^-)$ from $K[PF_6] = (7.7891 / 2) - 1.52 = 2.37$ Å

$r(PF_6^-)$ from $Rb[PF_6] = (7.887 / 2) - 1.66 = 2.28$ Å

$r(PF_6^-)$ from $Cs[PF_6] = (8.197 / 2) - 1.81 = 2.29$ Å

$r(PF_6^-) = (2.37 + 2.28 + 2.29) / 3 = 2.31$ Å

$r(N_1^+)$

$r(N_1^+)$ was obtained from the equation (3) using $r(PF_6^-) = 2.31$ Å:

$r(N_1^+) = (\sqrt{} \cdot 12.59 / 4) - 2.31 = 3.14$ Å

$r(N_2^+)$

$r(N_2^+)$ was obtained from the equation (2) using $r(PF_6^-) = 2.31$ Å:

$r(N_2^+) = (11.309 / 2) - 2.31 = 3.34$ Å

$r(P_2^+)$

$r(P_2^+)$ was obtained from the equation (2) using $r(PF_6^-) = 2.31$ Å:

$r(P_2^+) = (11.845 / 2) - 2.31 = 3.61$ Å

$r(N_3^+)$

$r(N_3^+)$ was obtained from the equation (2) using $r(PF_6^-) = 2.31$ Å:

$r(N_3^+) = (12.047 / 2) - 2.31 = 3.71$ Å

$r(P_3^+)$

$r(P_3^+)$ was obtained from the equation (2) using $r(PF_6^-) = 2.31$ Å:

$r(P_3^+) = [(9.702/\sqrt{})^2 + (12.9888/4)^2]^{1/2} - 2.31 = 4.16$ Å

$r(BF_4^-)$

$r(BF_4^-)$ was obtained from the *a* lattice parameters of $[N_2][BF_4]$ (10.827 Å) and $[P_2][BF_4]$ (11.331 Å) by analogy with equation (2):

$r(BF_4^-)$ from $[N_2][BF_4] = (10.827 / 2) - 3.34 = 2.07$ Å

$r(BF_4^-)$ from $[P_2][BF_4] = (11.331 / 2) - 3.61 = 2.06$ Å

where $r(N_2^+) = 3.34$ Å and $r(P_2^+) = 3.61$ Å were used.

The average of the two $r(BF_4^-)$ values from these two equations was 2.07 Å.

S-3. Synthesis of [P$_1$][BF$_4$]: The starting chloride, [P$_1$][Cl] (0.635 g, 4.98 mmol), dried under vacuum at 353 K was loaded in a PFA reactor in a drybox. A large excess of anhydrous HF (~2mL) was distilled onto [P$_1$][Cl] at 77 K under vacuum. On warming up to room temperature, the reaction proceeded and evolution of HCl was observed. The volatiles, HCl and excess HF, were removed by pumping at room temperature. This procedure (addition of large excess of anhydrous HF and elimination of the volatiles) was repeated once more to complete the reaction. Onto the obtained [P$_1$][(FH)$_n$F], anhydrous HF as a solvent (~ 2mL) was condensed at 77 K. After warming up the reactor to room temperature, excess BF$_3$ was introduced to the gas phase and the liquid phase was vigorously agitated for 3 h. The pressure inside the reactor was always monitored during this reaction and the uptake of BF$_3$ was confirmed. The volatiles were removed under vacuum at room temerapture for 1 h, at 323 K for 2 h, and at 353 K for 3h, giving [P$_1$][BF$_4$] as white powder (0.878 g, 4.94 mmol,). Raman (Figure S20) ($\tilde{v}$ / cm^{-1}, intensity): 765(m) (BF$_4^-$, v_1). Elemental analysis calcd (%) for C$_4$H$_{12}$PBF$_4$: C 49.68, H 9.73; found: C 49.67, H, 9.68.

Synthesis of [P$_1$][PF$_6$]: This compound was prepared in the same manner as for [P$_1$][BF$_4$], using [P$_1$][Cl] (0.444 g, 3.48 mmol) and PF$_5$ instead of BF$_3$, which gave [P$_1$][PF$_6$] as white powder (0.822 g, 3.48 mmol). Raman (Figure S21) ($\tilde{v}$ / cm^{-1}, intensity): 730(s) (PF$_6^-$, v_1), 564(w) (PF$_6^-$, v_2), 467(w) (PF$_6^-$, v_5). Elemental analysis calcd (%) for C$_4$H$_{12}$P$_2$F$_6$: C 20.36, H 5.09, F 48.31; found: C 20.17, H 5.00, F 48.48.

Synthesis of [N$_3$][PF$_6$]: The starting bromide, [N$_3$][Br] (1.33 g, 5.00 mmol), and K[PF$_6$] (1.01 g, 5.50 mmol) were agitated for 24 h in a polypropylene vessel containing CH$_2$Cl$_2$ as solvent. The precipitated KBr was separated from the solution by centrifuging and the supernatant was washed with water four times. Removal of Br$^-$ was confirmed by adding a 1M AgNO$_3$ aqueous solution to the separated water phase after final washing. The volatiles were removed under vacuum at 298 K, at 313 K, 333 K, and 353 K (1d for each temperature), giving [N$_3$][BF$_4$] as white powder (0.822 g,

1.906 mmol). Raman (Figure S22) ($\tilde{\nu}$ / cm^{-1}, intensity): 729(s) (PF$_6^-$, ν_1), 563(w) (PF$_6^-$, ν_2), 467(w) (PF$_6^-$, ν_5). Elemental analysis calcd (%) for C$_{12}$H$_{28}$NPF$_6$: C 43.50, H 8.52 N 4.23, F 34.41; found: C 43.28, H 8.47 N 4.20, F 34.67.

Synthesis of [P$_3$][BF$_4$]: This compound was prepared in the same manner as for [N$_3$][PF$_6$], using [P$_3$][Br] (1.42 g, 5.01 mmol) and K[BF$_4$] (0.630 g, 5.00 mmol), which gave [P$_3$][BF$_4$] as white powder (0.358 g, 1.23 mmol). Raman (Figure S23) (wavenumber / cm^{-1}, intensity): 765(m) (BF$_4^-$, ν_1). Elemental analysis calcd (%) for C$_{12}$H$_{28}$PBF$_4$: C 49.68, H 9.78; found: C 49.67, H 9.68.

Synthesis of [P$_3$][PF$_6$]: This compound was prepared in the same manner as for [N$_3$][PF$_6$], using [P$_3$][Br] (1.42 g, 5.01 mmol) and K[PF$_6$] (0.980 g, 5.32 mmol), which gave [P$_3$][PF$_6$] as white powder (1.420 g, 4.08 mmol). Raman (Figure S24) ($\tilde{\nu}$ / cm^{-1}, intensity): 738(s) (PF$_6^-$, ν_1), 564(w) (PF$_6^-$, ν_2), 467(w) (PF$_6^-$, ν_5). Elemental analysis calcd (%) for C$_{12}$H$_{28}$P$_2$F$_6$: C 41.41, H 8.05, F 32.75; found: C 41.20, H 8.30, F 32.63.

Table S1 Experimental and calculated d values (d_{obs} and d_{calc}), the corresponding $10^4 d^{-2}$ values, indices (h, k, and l), crystal system, lattice parameters (a, c, V), and the number of formula unit per unit cell (Z) for Phase I of [N$_n$][BF$_4$], [N$_n$][PF$_6$], [P$_n$][BF$_4$], and [P$_n$][PF$_6$]

[N$_1$][PF$_6$] (563 K)

h	K	l	d_{obs} / Å	d_{calc} / Å	$10^4 d_{obs}^{-2}$ / Å	$10^4 d_{calc}^{-2}$ / Å	I_{obs}
1	1	0	8.457	8.647	139.8	133.7	0.3
2	0	0	6.220	6.167	258.5	262.9	16.4
2	1	1	5.096	5.055	385.1	391.3	3.5
2	2	0	4.405	4.388	515.4	519.4	100.0
2	2	2	3.590	3.592	775.9	775.0	0.6
3	2	1	3.329	3.329	902.3	902.3	1.1
4	0	0	3.113	3.116	1031.9	1029.9	3.3
3	3	0	2.944	2.940	1153.8	1156.9	1.4
4	2	0	2.785	2.791	1289.3	1283.7	0.4

Cubic, a = 12.59(2) Å, V = 1995(5) Å^3, Z = 8.

[N$_2$][BF$_4$] (373 K)

h	K	l	d_{obs} / Å	d_{calc} / Å	$10^4 d_{obs}^{-2}$ / Å	$10^4 d_{calc}^{-2}$ / Å	I_{obs}
1	1	1	6.241	6.226	256.7	258.0	0.8
2	0	0	5.381	5.394	345.4	343.7	100.0
2	2	0	3.818	3.818	686.0	686.0	20.7
3	1	1	3.259	3.258	941.5	942.1	4.3
2	2	2	3.119	3.119	1027.9	1027.9	3.7

Cubic, a = 10.827(6) Å, V = 1269.1(12) Å^3, Z = 4.

[N$_2$][PF$_6$] (373 K)

h	k	l	d_{obs} / Å	d_{calc} / Å	$10^4 d_{obs}^{-2}$ / Å	$10^4 d_{calc}^{-2}$ / Å	I_{obs}
1	1	1	6.647	6.608	226.3	229.0	8.8
2	0	0	5.751	5.723	302.4	305.3	100.0
2	2	0	4.051	4.046	609.4	610.9	29.4
3	1	1	3.440	3.451	845.1	839.7	8.4
2	2	2	3.300	3.303	918.3	916.6	5.2

Cubic, a = 11.309(2) Å, V = 1446.3(4) Å^3, Z = 4.

[P$_2$][BF$_4$] (473 K)

h	k	l	d_{obs} / Å	d_{calc} / Å	$10^4 d_{obs}^{-2}$ / Å	$10^4 d_{calc}^{-2}$ / Å	I_{obs}

h	k	l	d_{obs} / Å	d_{calc} / Å	$10^4 d_{obs}^{-2}$ / Å	$10^4 d_{calc}^{-2}$ / Å	I_{obs}
1	1	1	6.585	6.591	230.6	230.2	2.5
2	0	0	5.718	5.702	305.9	307.6	100.0
2	2	0	4.016	4.024	620.0	617.6	24.3
3	1	1	3.424	3.430	853.0	850.0	2.7
2	2	2	3.291	3.283	923.3	927.8	2.7

Cubic, $a = 11.331(11)$ Å, $V = 1455(2)$ Å^3, $Z = 4$.

[P$_2$][PF$_6$] (498 K)

h	k	l	d_{obs} / Å	d_{calc} / Å	$10^4 d_{obs}^{-2}$ / Å	$10^4 d_{calc}^{-2}$ / Å	I_{obs}
1	1	1	6.845	6.842	213.4	213.6	7.2
2	0	0	5.922	5.925	285.1	284.9	100.0
2	2	0	4.188	4.189	570.1	569.9	26.7
3	1	1	3.574	3.572	782.9	783.7	3.4
2	2	2	3.419	3.420	855.5	855.0	3.4

Cubic, $a = 11.845(2)$ Å, $V = 1661.7(5)$ Å^3, $Z = 4$.

[N$_3$][BF$_4$] (453 K)

h	k	l	d_{obs} / Å	d_{calc} / Å	$10^4 d_{obs}^{-2}$ / Å	$10^4 d_{calc}^{-2}$ / Å	I_{obs}
1	1	0	9.787	9.788	104.4	104.4	100.0
2	0	0	6.960	6.962	206.4	206.3	6.9
2	1	0	6.247	6.237	256.2	257.1	2.5
2	1	1	5.692	5.700	308.7	307.8	17.0
2	2	0	4.947	4.944	408.6	409.1	30.2
3	1	0	4.421	4.427	511.6	510.2	2.6
2	2	2	4.047	4.045	610.6	611.2	7.7
3	2	0	3.889	3.886	661.2	662.2	14.8
3	2	1	3.754	3.747	709.6	712.3	11.2
4	0	0	3.502	3.507	815.4	813.1	3.7
3	3	0	3.306	3.308	914.9	913.8	4.4

Cubic, $a = 14.129(6)$ Å, $V = 2820(2)$ Å^3, $Z = 6$.

[N$_3$][PF$_6$] (493 K)

h	k	l	d_{obs} / Å	d_{calc} / Å	$10^4 d_{obs}^{-2}$ / Å	$10^4 d_{calc}^{-2}$ / Å	I_{obs}
1	1	0	8.374	8.418	142.6	141.1	72.6
1	1	1	6.887	6.888	210.8	210.8	10.2
2	0	0	6.028	5.973	275.2	280.3	59.7
2	1	1	4.882	4.885	419.6	419.1	100.0
2	2	0	4.212	4.234	563.7	557.8	32.3

2	2	1	3.975	3.993	632.9	627.2	32.3
3	1	0	3.788	3.790	696.9	696.2	25.0
3	1	1	3.622	3.614	762.3	765.6	2.8
2	2	2	3.462	3.461	834.3	834.8	2.7

Cubic, $a = 12.047(16)$ Å, $V = 1748(4)$ Å^3, $Z = 4$.

[P$_3$][BF$_4$] (423 K)

h	k	l	d_{obs} / Å	d_{calc} / Å	$10^4 d_{obs}^{-2}$ / Å	$10^4 d_{calc}^{-2}$ / Å	I_{obs}
1	1	0	10.159	10.175	96.9	96.6	100.0
2	0	0	7.197	7.181	193.1	193.9	7.8
2	1	0	6.427	6.420	242.1	242.6	7.2
2	1	1	5.847	5.859	292.5	291.3	20.8
2	2	0	5.074	5.071	388.4	388.9	40.7
3	1	0	4.531	4.534	487.1	486.4	4.3
2	2	2	4.134	4.138	585.1	584.0	8.5
3	2	0	3.979	3.975	631.6	632.9	41.5
3	2	1	3.836	3.830	679.6	681.7	23.5
4	0	0	3.579	3.582	780.7	779.4	9.5
3	3	0	3.368	3.377	881.6	876.9	8.8

Cubic, $a = 14.298(6)$ Å, $V = 2923(2)$ Å^3, $Z = 6$.

[P$_3$][PF$_6$] (473 K)

h	k	l	d_{obs} / Å	d_{calc} / Å	$10^4 d_{obs}^{-2}$ / Å	$10^4 d_{calc}^{-2}$ / Å	I_{obs}
1	0	0	8.281	8.287	145.8	145.6	100.0
1	0	1	6.965	6.958	206.1	206.6	1.1
0	0	2	6.379	6.376	245.8	246.0	21.0
1	0	2	5.064	5.071	390.0	388.9	9.7
1	1	0	4.816	4.813	431.1	431.7	30.6
2	0	0	4.173	4.173	574.3	574.3	10.6
2	0	1	3.965	3.969	636.1	634.8	9.7
1	1	2	3.855	3.851	672.9	674.3	3.6

Hexagonal, $a = 9.702(4)$ Å, $c = 12.888(11)$ Å, $V = 1050.7(11)$ Å^3, $Z = 2$.

[N$_4$][BF$_4$] (413 K)

H	k	l	d_{obs} / Å	d_{calc} / Å	$10^4 d_{obs}^{-2}$ / Å	$10^4 d_{calc}^{-2}$ / Å	I_{obs}
1	1	0	10.657	10.677	88.1	87.7	100.0
2	0	0	7.554	7.527	175.2	176.5	4.8
2	1	0	6.738	6.736	220.3	220.4	5.9

h	k	l	d_{obs} / Å	d_{calc} / Å	$10^4 d_{obs}^{-2}$ / Å	$10^4 d_{calc}^{-2}$ / Å	I_{obs}
2	1	1	6.153	6.143	264.1	265.0	14.6
2	2	0	5.342	5.319	350.4	353.5	14.9
3	1	0	4.757	4.759	441.9	441.5	1.4
2	2	2	4.342	4.341	530.4	530.7	23.8
3	2	0	4.167	4.169	575.9	575.4	13.6
3	2	1	4.02	4.019	618.8	619.1	6.5
4	0	0	3.751	3.755	710.7	709.2	6.4
3	3	0	3.539	3.540	798.4	798.0	3.0

Cubic, a = 14.971(8) Å, V = 3353(3) Å³, Z = 6.

[N₄][PF₆] (413 K)

h	k	l	d_{obs} / Å	d_{calc} / Å	$10^4 d_{obs}^{-2}$ / Å	$10^4 d_{calc}^{-2}$ / Å	I_{obs}
1	1	0	10.827	10.824	85.3	85.4	100.0
2	0	0	7.666	7.661	170.2	170.4	6.6
2	1	0	6.851	6.854	213.1	212.9	3.8
2	1	1	6.258	6.258	255.3	255.3	12.9
2	2	0	5.420	5.421	340.4	340.3	15.1
3	1	0	4.849	4.849	425.3	425.3	4.9
2	2	2	4.429	4.427	509.8	510.2	17.3
3	2	0	4.253	4.254	552.9	552.6	16.1
3	2	1	4.099	4.099	595.2	595.2	8.6
4	0	0	3.835	3.835	679.9	679.9	3.7
3	3	0	3.616	3.616	764.8	764.8	1.5

Cubic, a = 15.3538(13) Å, V = 3619.5(5) Å³, Z = 6.

[P₄][BF₄] (348 K)

h	k	l	d_{obs} / Å	d_{calc} / Å	$10^4 d_{obs}^{-2}$ / Å	$10^4 d_{calc}^{-2}$ / Å	I_{obs}
1	1	0	10.608	10.623	88.9	88.6	100.0
2	0	0	7.538	7.523	176.0	176.7	5.1
2	1	0	6.743	6.731	219.9	220.7	8.7
2	1	1	6.129	6.146	266.2	264.7	14.0
2	2	0	5.317	5.325	353.7	352.7	21.2
3	1	0	4.765	4.764	440.4	440.6	8.7
2	2	2	4.362	4.35	525.6	528.5	31.3
3	2	0	4.179	4.179	572.6	572.6	10.0
3	2	1	4.023	4.028	617.9	616.3	12.3
4	0	0	3.766	3.768	705.1	704.3	3.8
3	3	0	3.560	3.553	789.0	792.2	3.1

Cubic, $a = 15.097(8)$ Å, $V = 3440(3)$ Å^3, $Z = 6$.

[P$_4$][PF$_6$] (338 K)							
h	k	l	d_{obs} / Å	d_{calc} / Å	$10^4 d_{obs}^{-2}$ / Å	$10^4 d_{calc}^{-2}$ / Å	I_{obs}
1	1	0	10.782	10.814	86.0	85.5	75.1
2	0	0	7.670	7.650	170.0	170.9	13.4
2	1	0	6.849	6.843	213.2	213.6	5.1
2	1	1	6.247	6.247	256.2	256.2	51.6
2	2	0	5.405	5.411	342.3	341.5	82.5
3	1	0	4.835	4.840	427.8	426.9	22.6
2	2	2	4.421	4.418	511.6	512.3	100.0
3	2	0	4.247	4.245	554.4	554.9	79.7
3	2	1	4.098	4.091	595.5	597.5	66.4
4	0	0	3.820	3.827	685.3	682.8	24.0
3	3	0	3.608	3.608	768.2	768.2	12.0

Cubic, $a = 15.315(7)$ Å, $V = 3592(3)$ Å^3, $Z = 6$.

Table S2 Experimental and calculated d values (d_{obs} and d_{calc}), the corresponding 10^4d^{-2} values, indices (h, k, and l), crystal system, lattice parameters (a, c, V), and the number of formula unit per unit cell (Z) for Phase II of [N$_1$][PF$_6$]

[N$_1$][PF$_6$] (298 K)

h	k	l	d_{obs} / Å	d_{calc} / Å	$10^4d_{obs}^{-2}$ / Å	$10^4d_{calc}^{-2}$ / Å	I_{obs}
1	1	0	8.30	8.38	145.2	142.4	1.3
0	0	1	5.99	6.10	278.7	268.7	24.8
1	0	1	4.97	4.96	404.8	406.5	13.8
1	1	1	4.31	4.29	538.3	543.4	100.0
2	1	1	3.25	3.24	946.7	952.6	6.2
0	0	2	3.08	3.08	1054.1	1054.1	0.4
2	2	0	3.01	3.02	1103.7	1096.4	3.3
1	0	2	2.90	2.90	1189.1	1189.1	4.1
2	2	1	2.70	2.71	1371.7	1361.6	1.2
3	0	1	2.59	2.59	1490.7	1490.7	2.8

Tetragonal, $a = 8.625(10)$ Å, $c = 6.227(8)$ Å, $V = 463.2(9)$ Å^3, $Z = 2$

Table S3 Crystallographic data and refinement results for [P4][PF6] at 113, 243, and 273 K.

	[P4][PF6] at 113 K	[P4][PF6] at 243 K	[P4][PF6] at 273 K
Formula	$C_{16}H_{36}F_6P_2$	$C_{16}H_{36}F_6P_2$	$C_{16}H_{36}F_6P_2$
Fw	404.39	404.39	404.39
crystal size, mm	0.20×0.20×0.60	0.20×0.20×0.60	0.20×0.20×0.60
T/K	113	243	273
crystal system	monoclinic	monoclinic	orthorhombic
space group	$P2_1/c$	$P2_1/c$	$Pmcn$
a/Å	9.7465(2)	9.8567(12)	9.9807(9)
b/Å	14.0652(4)	14.1385(17)	13.8901(15)
c/Å	15.5029(4)	15.777(2)	16.2367(16)
β/deg	93.2170(10)	92.422(3)	−
V/Å^3	2121.89(9)	2196.6(5)	2250.9(4)
Z	4	4	4
ρ_{calcd}/g cm^{-3}	1.266	1.223	1.193
$2\theta_{max}$/deg	54.96	54.96	54.96
Data completeness	0.998	0.998	0.998
F(000)	864	864	864
μ/mm^{-1}	0.252	0.243	0.237
λ/Å	0.71073	0.71073	0.71073
T_{min}/T_{max}	1.000/0.829	1.000/0.875	1.000/0.626
No. reflns collected, unique	20375, 4863	20860, 5030	21352, 2715
No. reflns in refinement	4863	5030	2715
No. parameters, restraints	221, 0	298, 255	197, 107
R_{int}	0.0192	0.0523	0.0249
$R_1(F_o)^a$	0.0398	0.0624	0.0951
$wR_2(F_o^2)^b$	0.1041	0.1840	0.3034
Goodness-of-fit on F^2	1.060	1.098	1.137
Largest difference peak, hole / e Å^{-3}	0.679, −0.385	0.575, −0.377	0.513, −0.308
CCDC No.	1010901	1010902	1010903

^{a} $R_1 = \sum||F_o| - |F_c|| / \sum|F_o|$ for $I > 2\sigma(I)$. ^{b} $wR_2 = \{\sum[w(F_o^2 - F_c^2)^2] / \sum[w(F_o^2)^2]\}^{1/2}$ for $I > 2\sigma(I)$.

Table S4 Crystallographic data and refinement results for $[P_4][PF_6]$ at 333 K.[a]

	$[P_4][PF_6]$ at 333 K
Formula	$C_{16}H_{36}F_6P_2$
Fw	404.39
crystal size, mm	0.10×0.10×0.10
T/K	333
crystal system	Cubic
space group	$Pm-3n$
a/Å	15.142(17)
V/Å^3	3472(7)
Z	6
ρ_{calcd}/g cm^{-3}	1.161
$2\theta_{max}$/deg	29.92
Data completeness	0.979
F(000)	1296
μ/mm^{-1}	0.231
λ/Å	0.71073
T_{min}/T_{max}	0.004, 1.000
No. reflns collected, unique	8698, 143
No. reflns in refinement	143
No. parameters, restraints	16, 9
R_{int}	0.183
$R_1(F_o)$[b]	0.3071
$wR_2(F_o{}^2)$[c]	0.6570
Goodness-of-fit on F^2	1.812
Largest differencce peak, hole / e Å^{-3}	0.229, −0.174

[a]The structure was not fully solved and refined due to the highly disordered structure at 333 K. [b] $R_1 = \sum ||F_o| - |F_c|| / \sum |F_o|$ for $I > 2\sigma(I)$. [c] $wR_2 = \{\sum[w(F_o{}^2 - F_c{}^2)^2] / \sum[w(F_o{}^2)^2]\}^{1/2}$ for $I > 2\sigma(I)$.
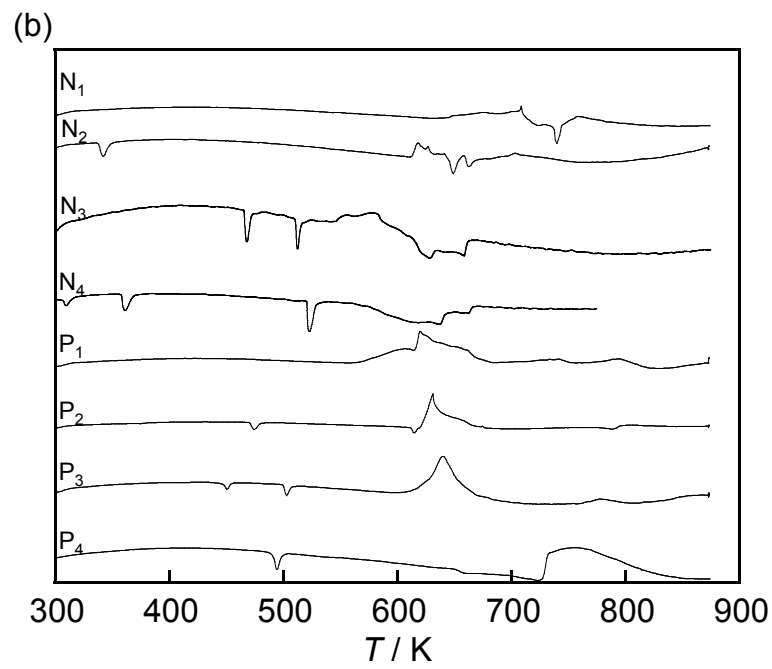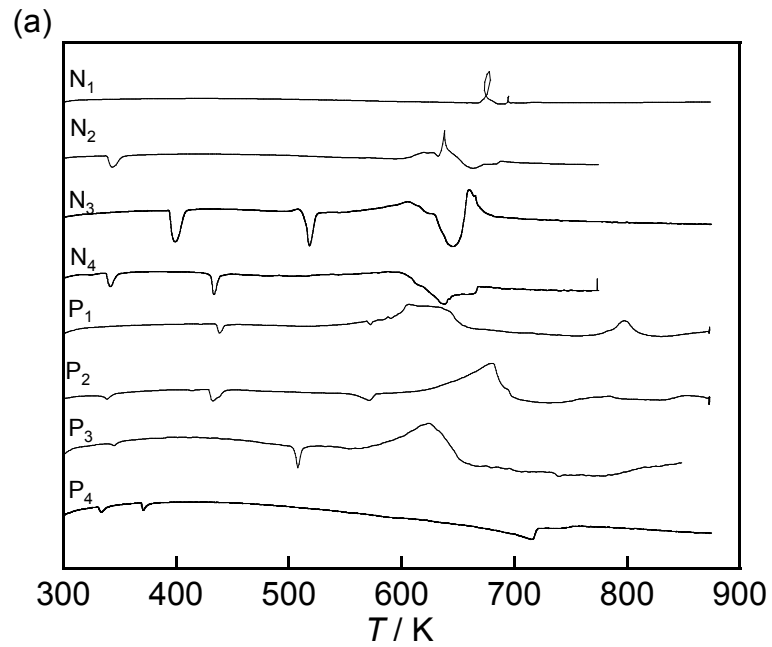
Figure S1 Differential thermal analysis curves for (a) $[N_n][BF_4]$ and $[P_n][BF_4]$ and (b) $[N_n][PF_6]$ and $[P_n][PF_6]$. Scan rate: 5 K min^{-1}.
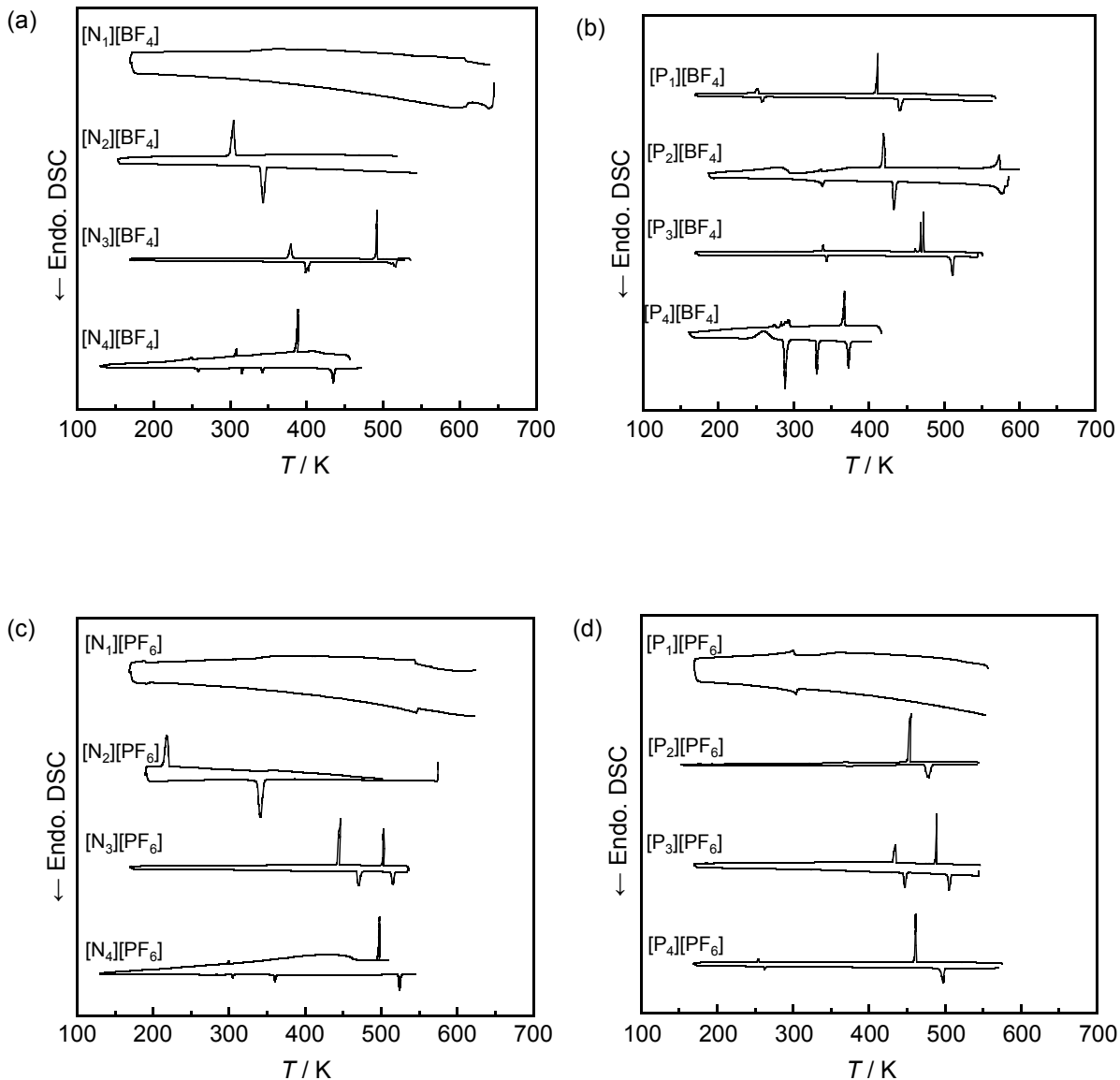
Figure S2 Differential scanning calorimetric curves of (a) $[N_n][BF_4]$, (b) $[P_n][BF_4]$, (c) $[N_n][PF_6]$, and (d) $[P_n][PF_6]$. Scan rate: 5 K min^{-1}.
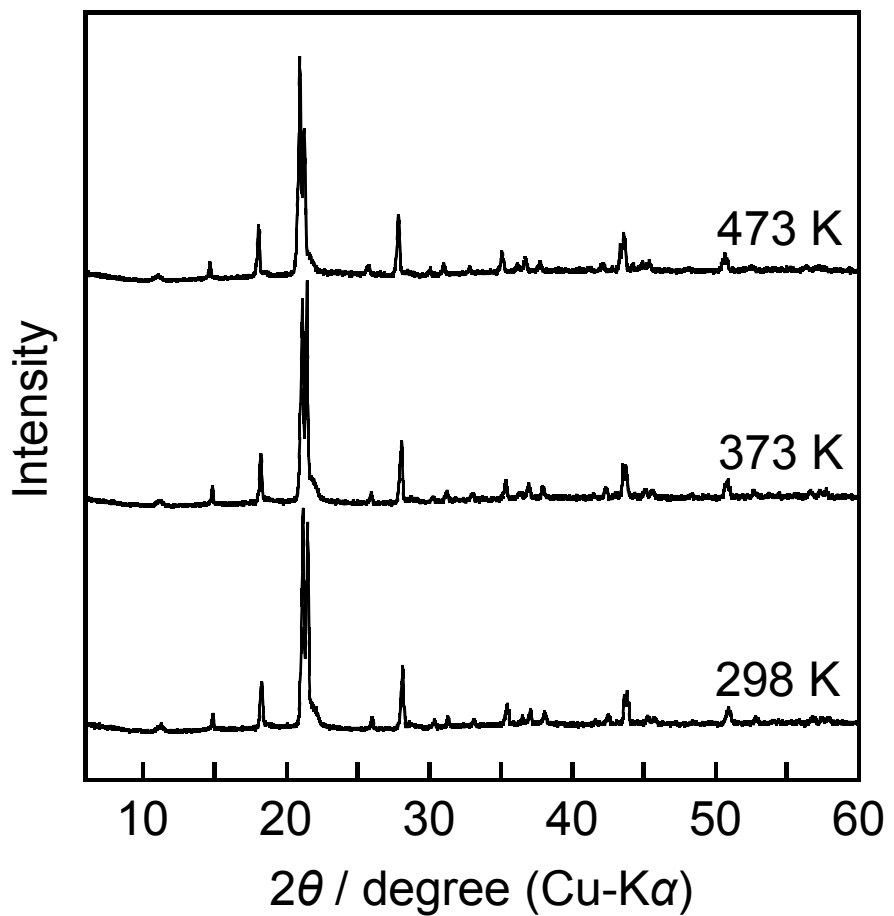
Figure S3 Powder XRD patterns of Phase II at 473 K, Phase II at 373 K, and Phase II at 298 K for [N$_1$][BF$_4$].
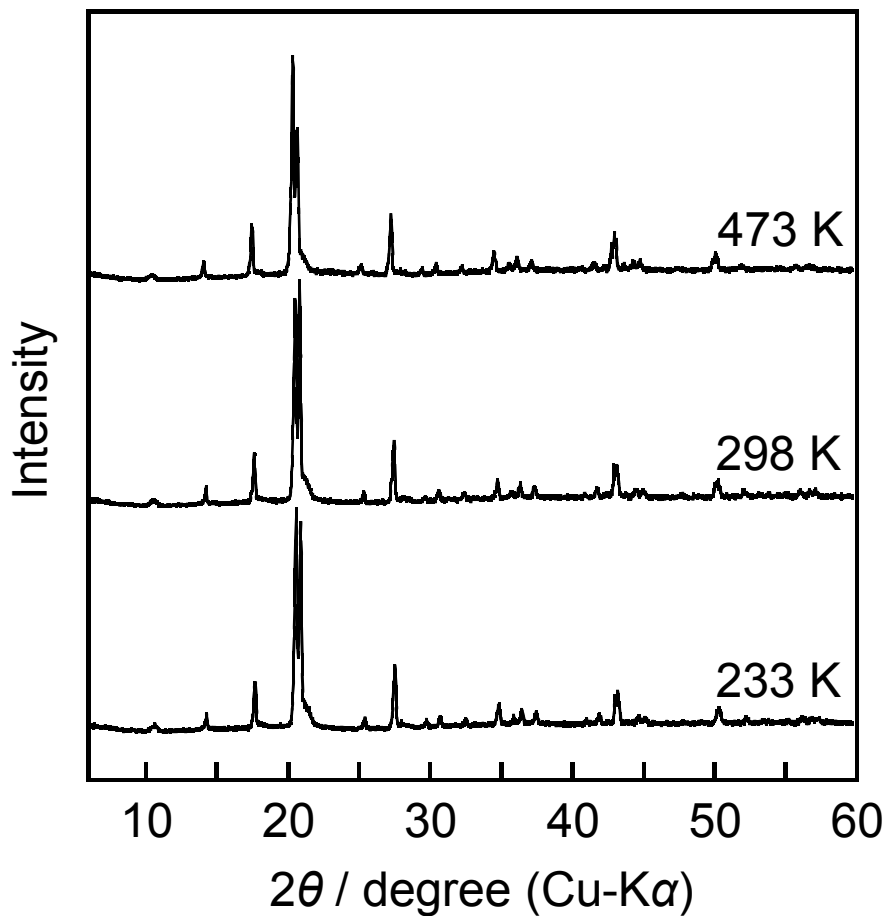
Figure S4 Powder XRD patterns of (a) Phase II at 473 K, (b) Phase III at 298 K, and (c) Phase IV at 233 K for $[P_1][BF_4]$.
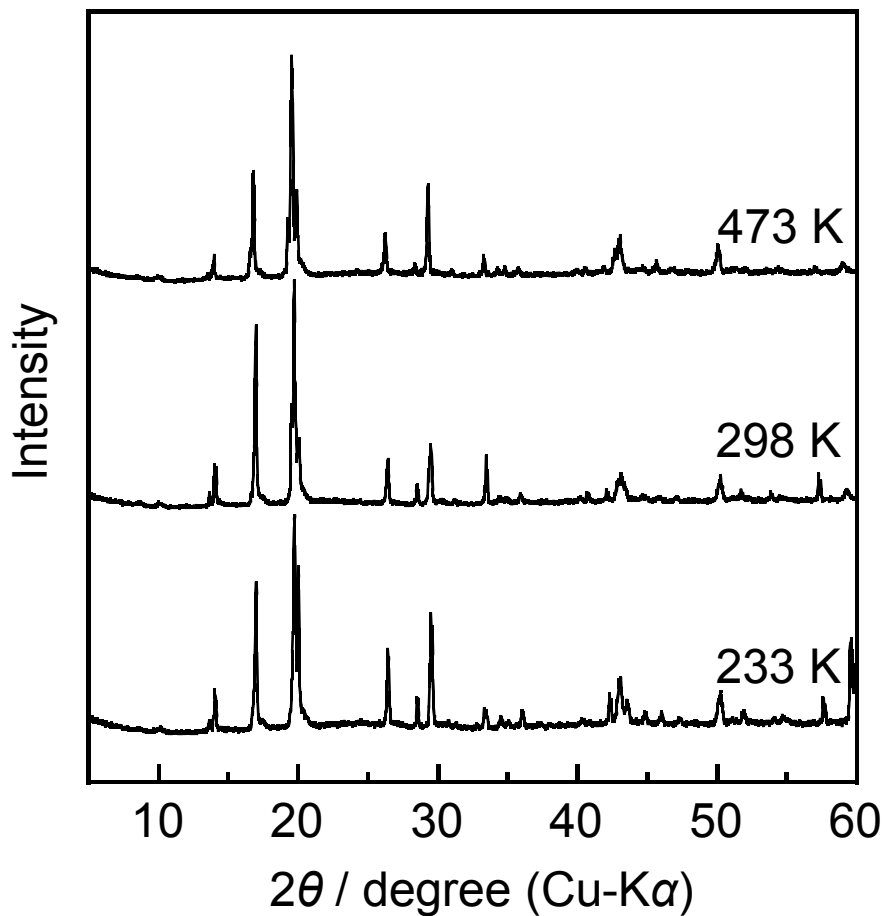
Figure S5 Powder XRD patterns of (a) Phase II at 473 K, (b) Phase III at 298 K, and (c) Phase III at 233 K for $[P_1][PF_6]$.
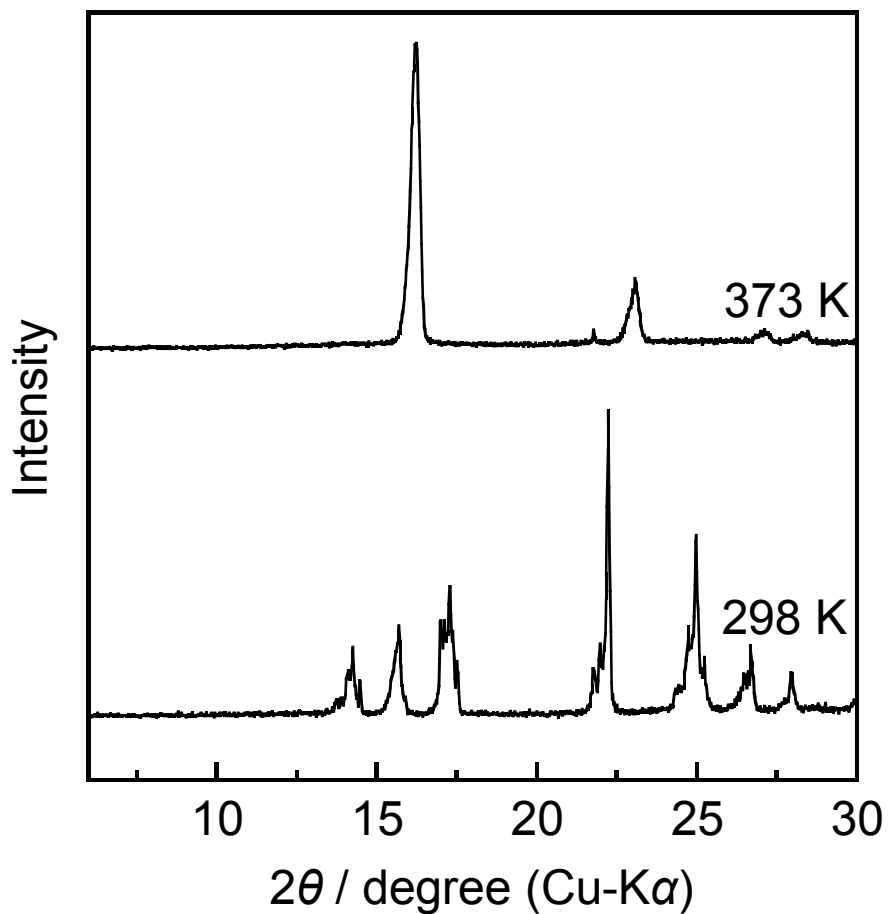
Figure S6 Powder XRD patterns of (a) Phase I at 373 K and (b) Phase II at 298 K for $[N_2][BF_4]$.
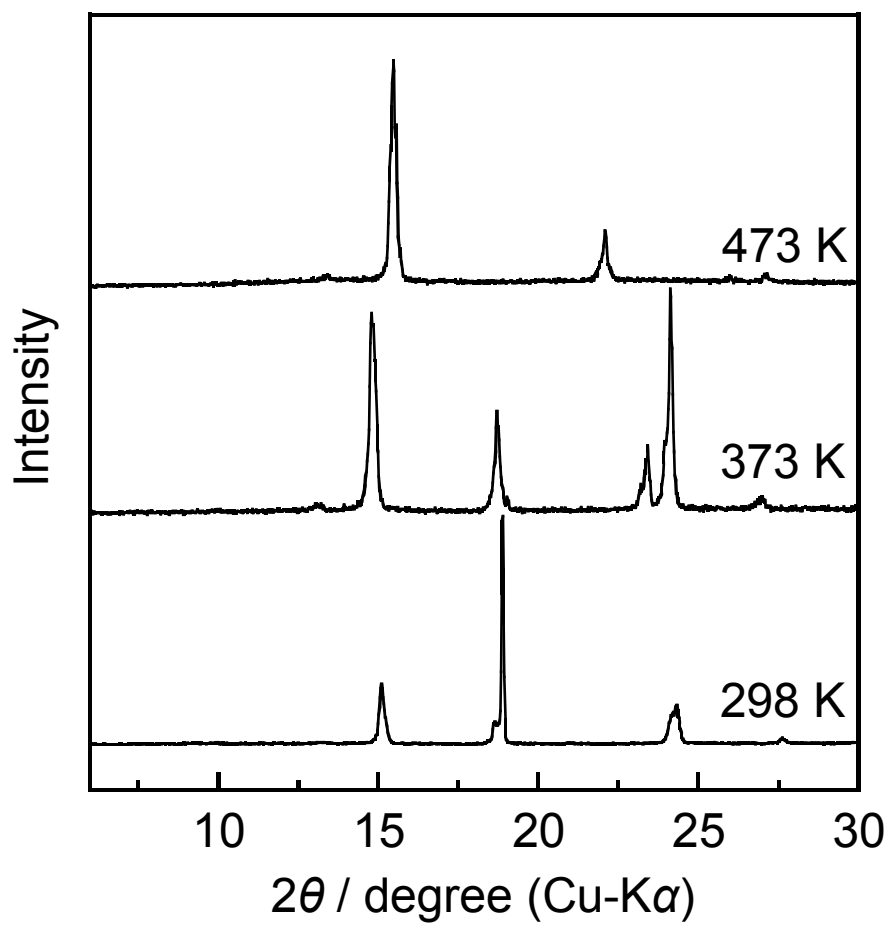
Figure S7 Powder XRD patterns of (a) Phase I at 473 K, (b) Phase II at 373 K, and (c) Phase III at 298 K for $[P_2][BF_4]$.
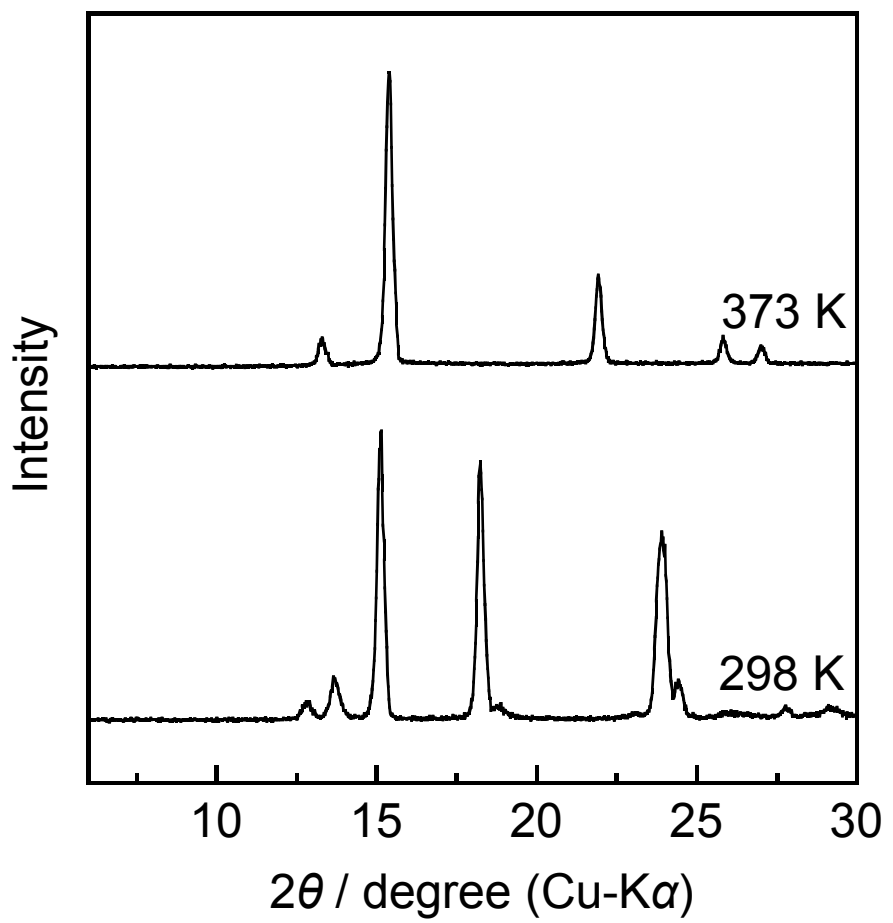
Figure S8 Powder XRD patterns of Phase I at 373 K and Phase II at 298 K for $[N_2][PF_6]$.
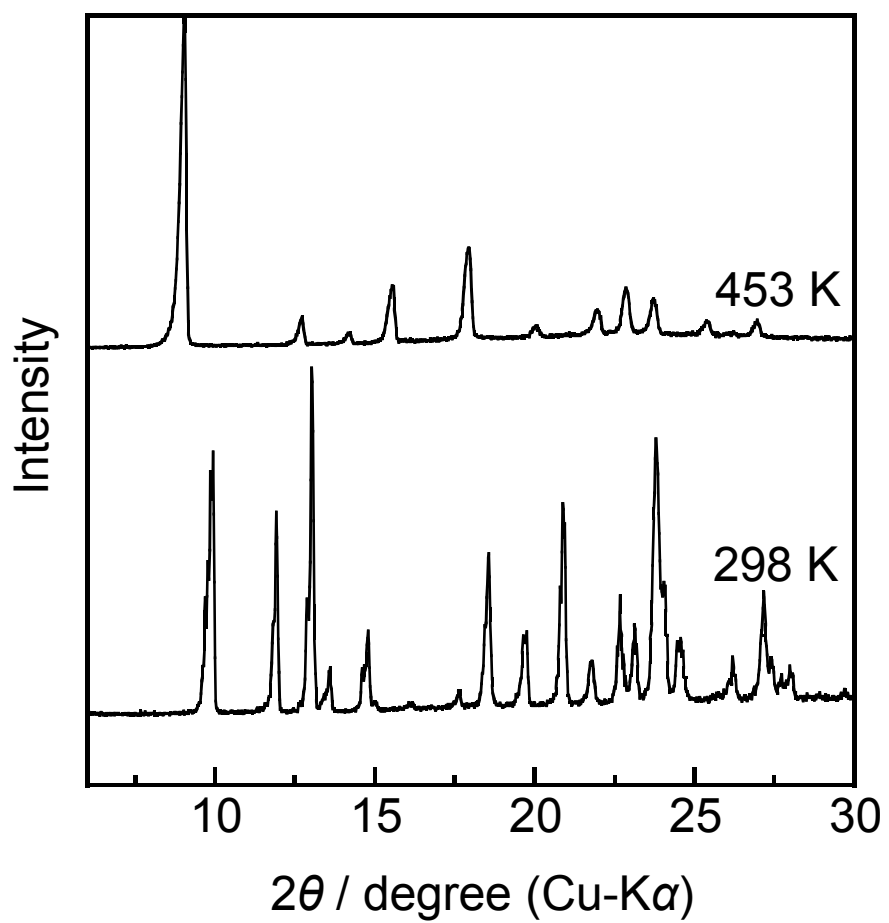
Figure S9 Powder XRD patterns of Phase I at 453 K and Phase II at 298 K for [N$_3$][BF$_4$].
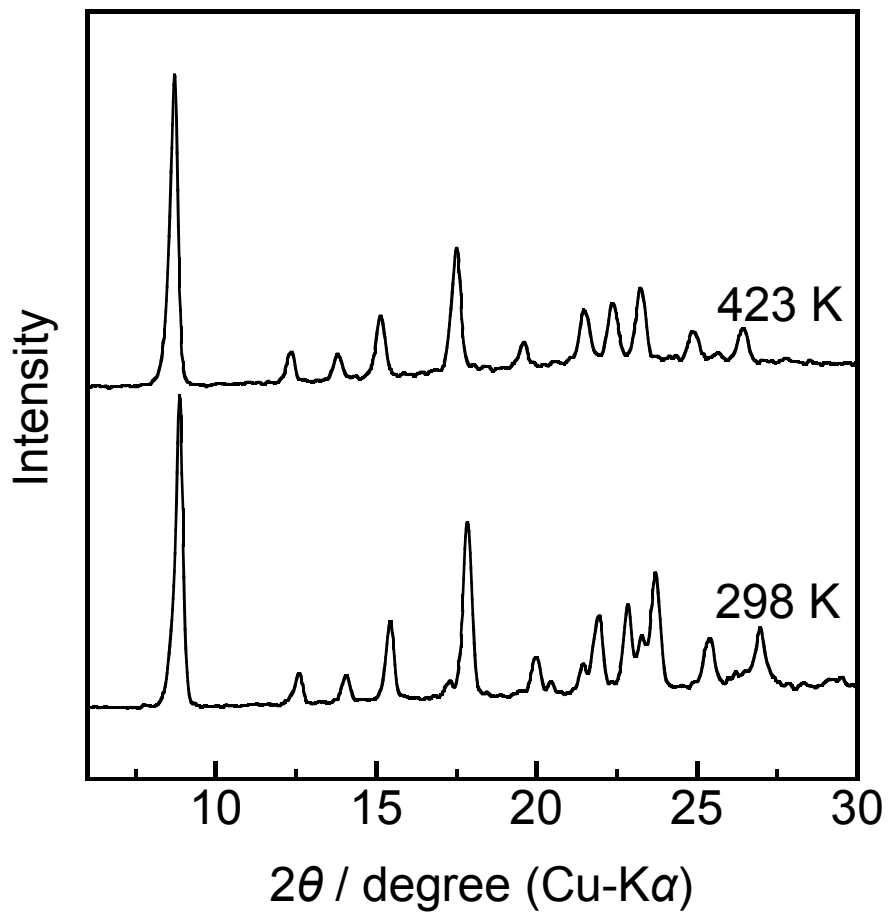
Figure S10 Powder XRD patterns of (a) Phase I at 423 K and (b) Phase II at 298 K for $[P_3][BF_4]$.
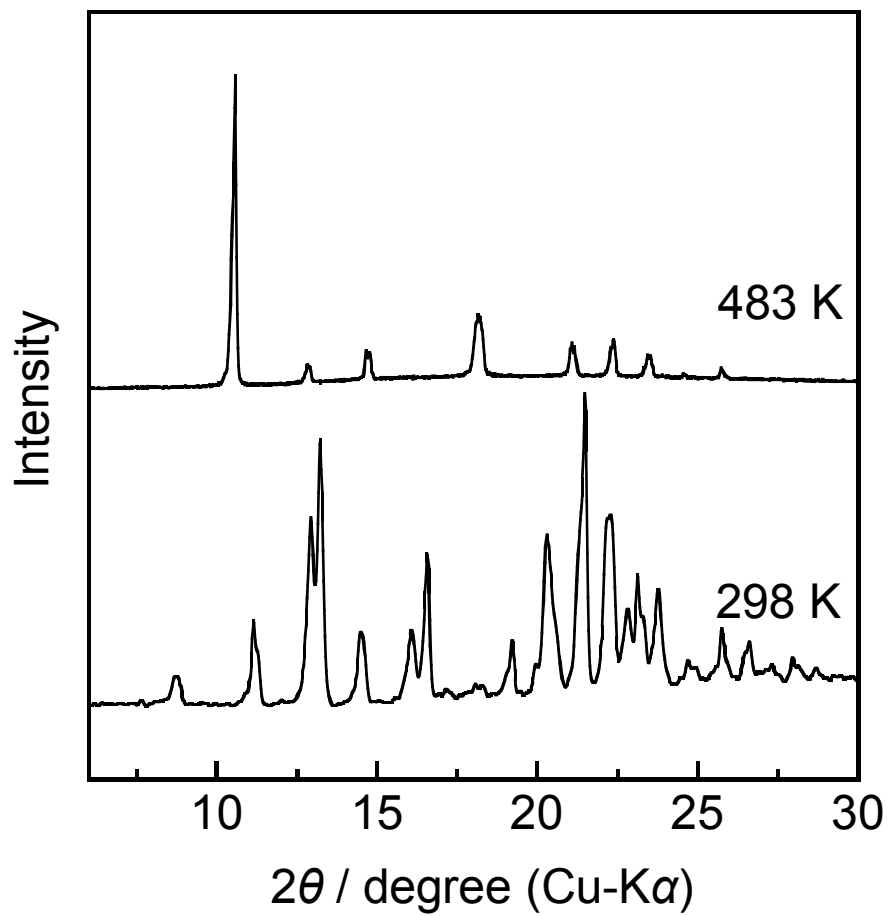
Figure S11 Powder XRD patterns of Phase I at 483 K and Phase II at 298 K for [N$_3$][PF$_6$].
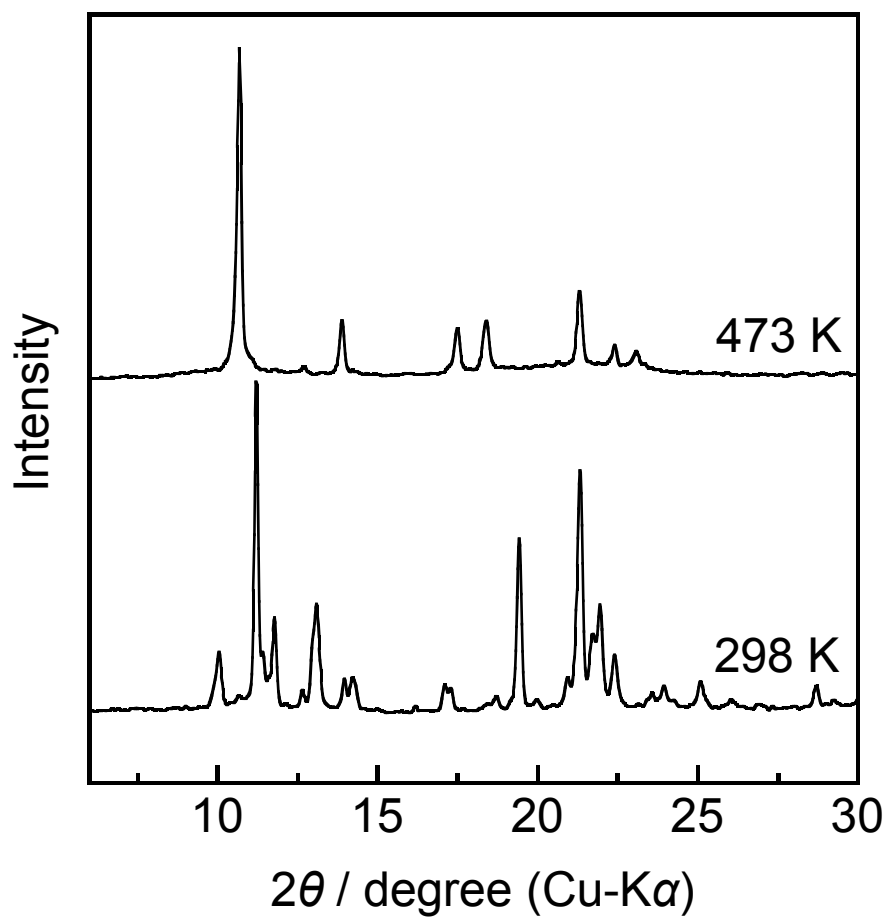
Figure S12 Powder XRD patterns of (a) Phase I at 473 K and (b) Phase II at 298 K for $[P_3][PF_6]$.
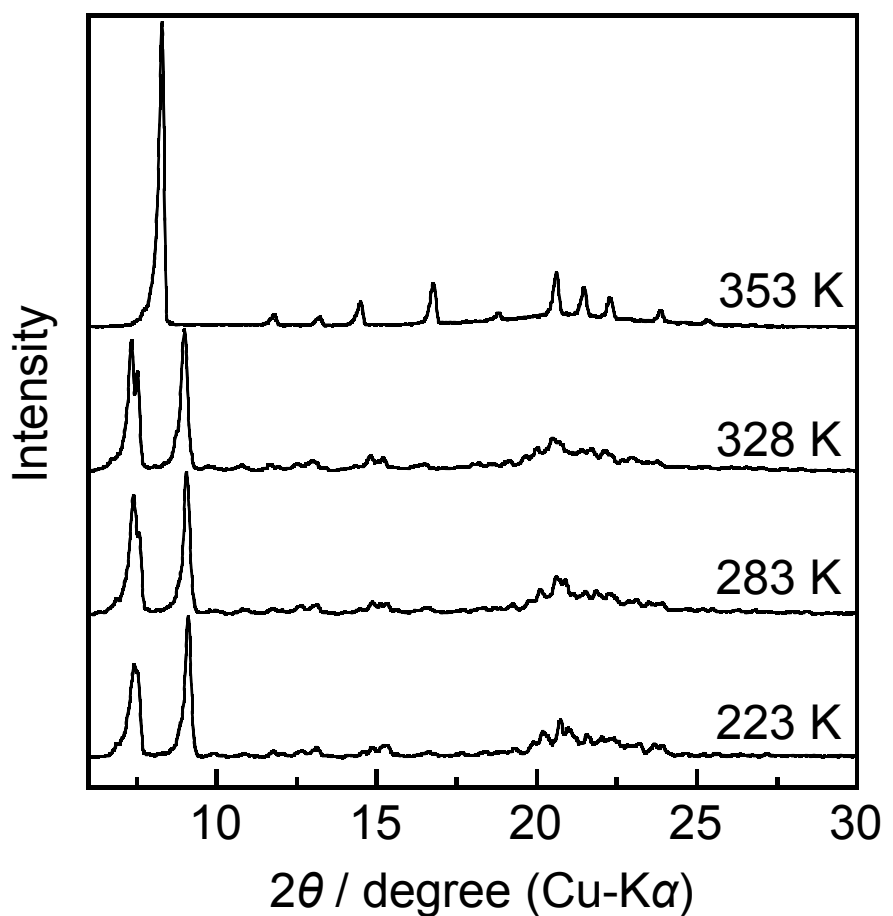
Figure S13 Powder XRD patterns of Phase I at 353 K, Phase II at 328 K, Phase III at 283 K, and Phase IV at 223 K for [N$_4$][BF$_4$].
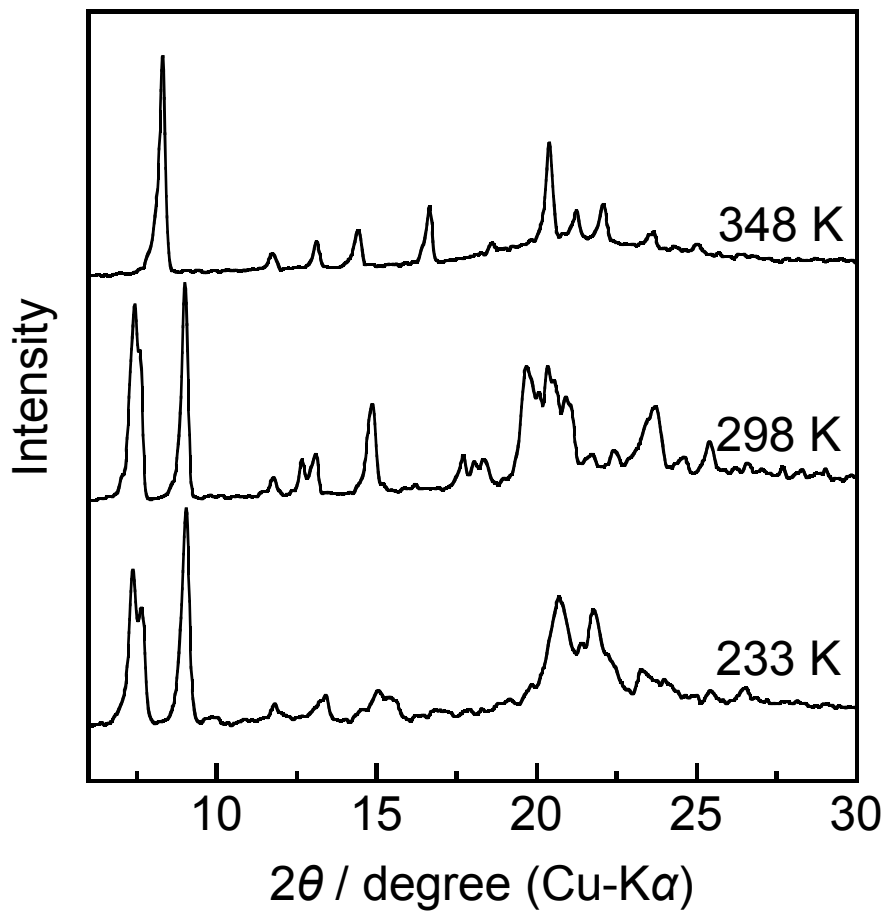
Figure S14 Powder XRD patterns of Phase I at 348 K, Phase II at 298 K, and Phase III at 233 K for [P$_4$][BF$_4$].
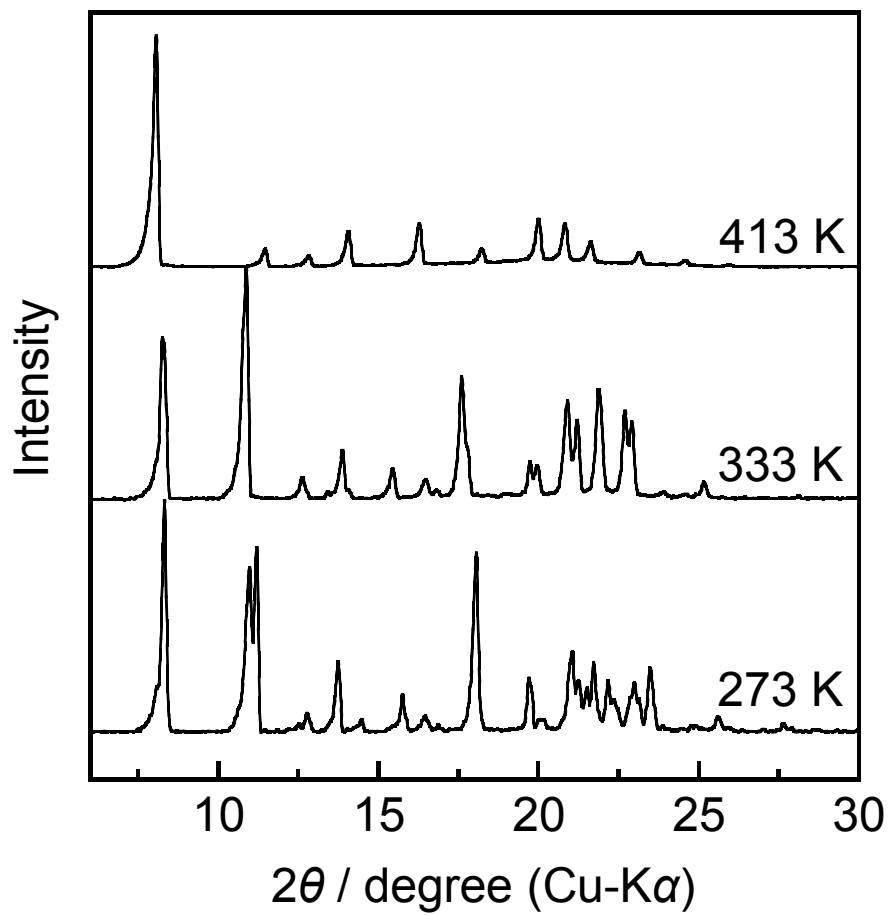
Figure S15 Powder XRD patterns of Phase I at 413 K, Phase II at 333 K, and Phase III at 273 K for [N$_4$][PF$_6$].
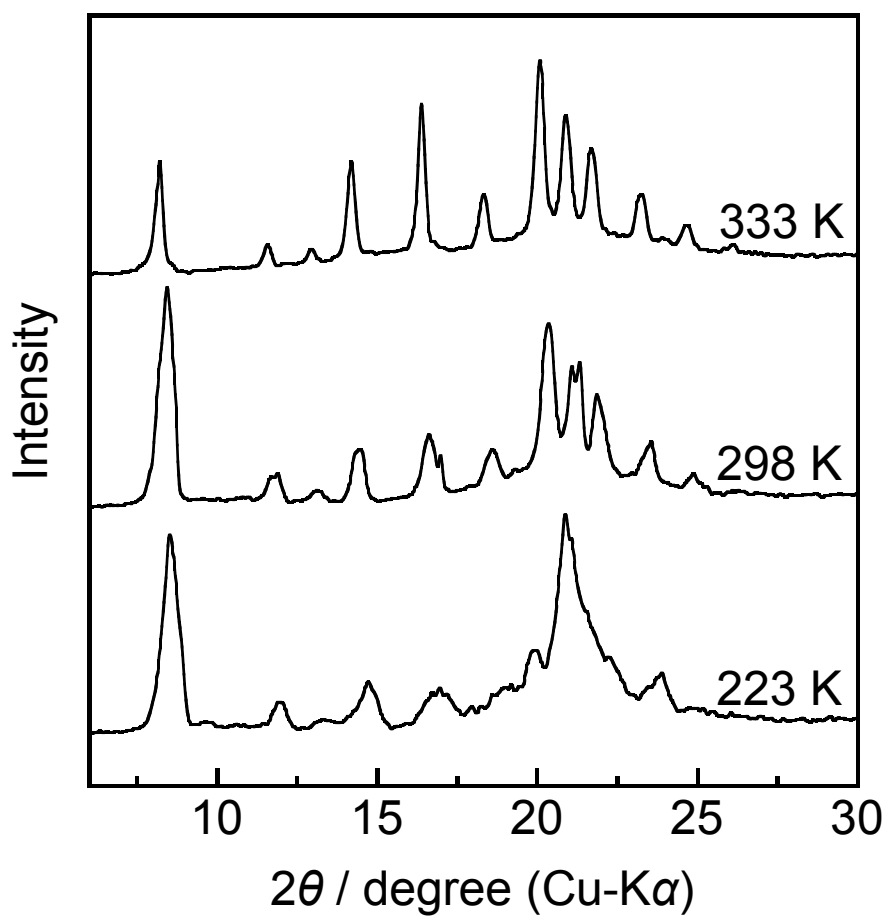
Figure S16 Powder XRD patterns of Phase I at 333 K, Phase II at 298 K, and Phase III at 223 K for [P$_4$][PF$_6$].
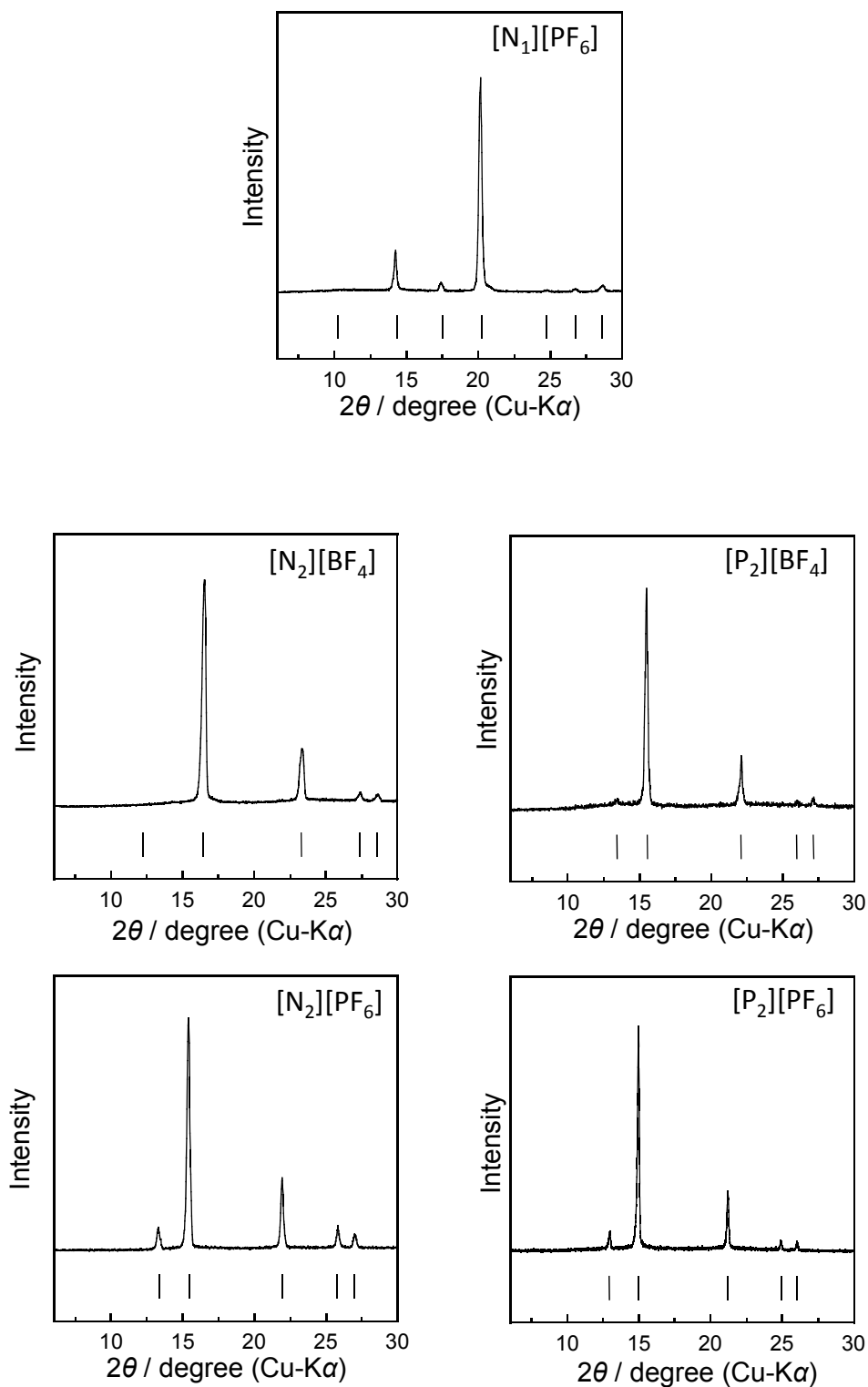
Figure S17 Powder XRD patterns of Phase I for [N$_1$][PF$_6$] (563 K), [N$_2$][BF$_4$] (373 K), [P$_2$][BF$_4$] (473 K), [N$_2$][PF$_6$] (373 K), and [P$_2$][PF$_6$] (498 K). Calculated peak positions are shown by bars at the bottom (see Table S1 for detailed XRD data).
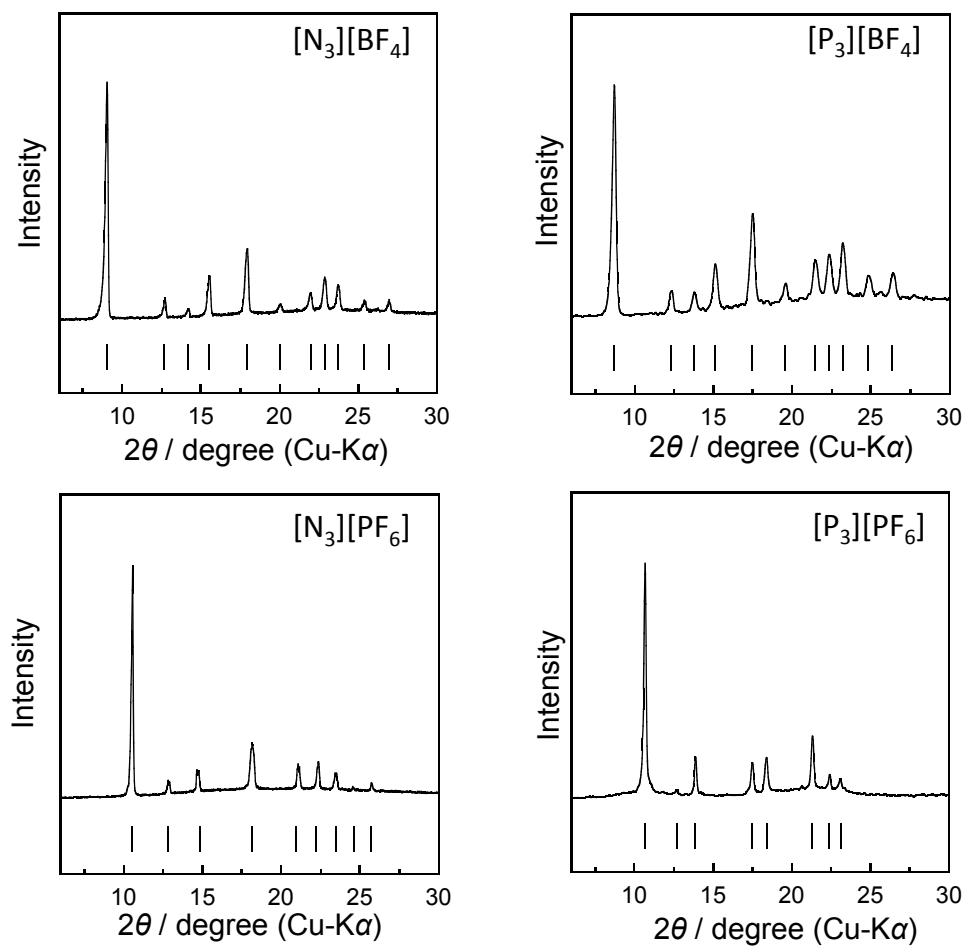
Figure S18 Powder XRD pattern of Phase I for $[N_3][BF_4]$ (453 K), $[P_3][BF_4]$ (423 K), $[N_3][PF_6]$ (493 K), and $[P_3][PF_6]$ (473 K). Calculated peak positions are shown by bars at the bottom (see Table S1 for detailed XRD data).
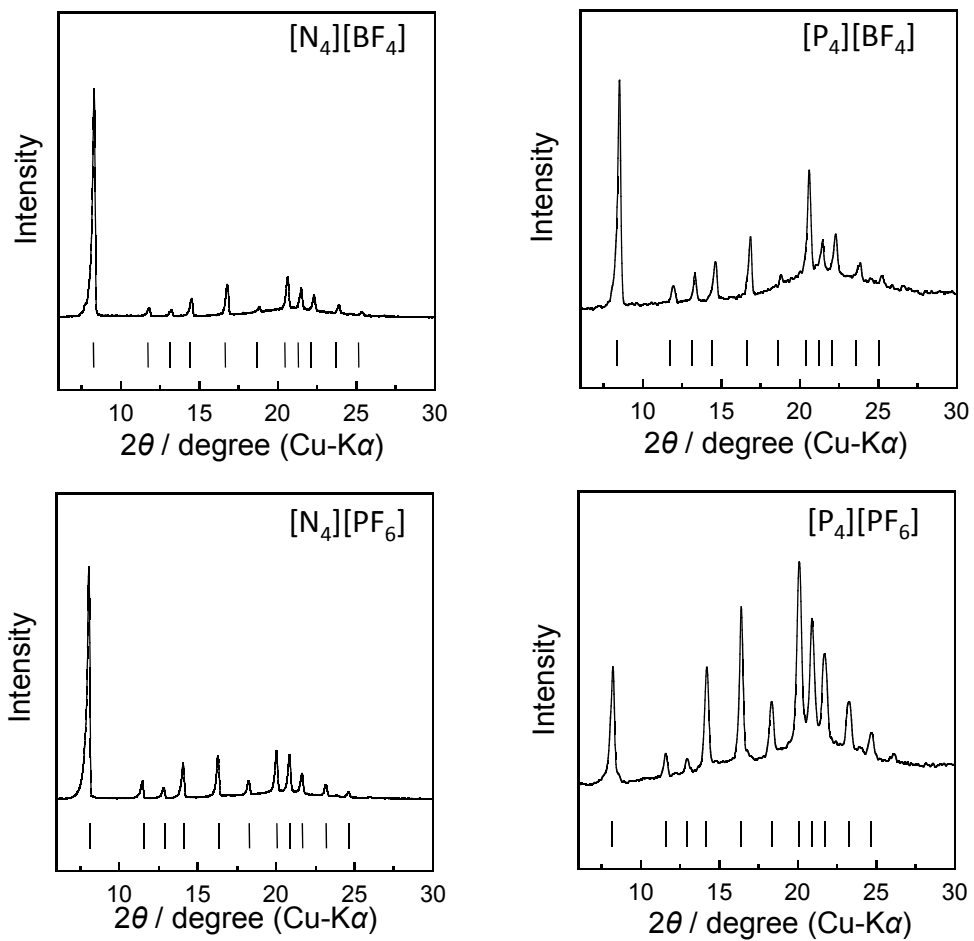
Figure S19 Powder XRD pattern of Phase I for [N$_4$][BF$_4$] (413 K), [P$_4$][BF$_4$] (348 K), [N$_4$][PF$_6$] (413 K), and [P$_4$][PF$_6$] (338 K). Calculated peak positions are shown by bars at the bottom (see Table S1 for detailed XRD data).
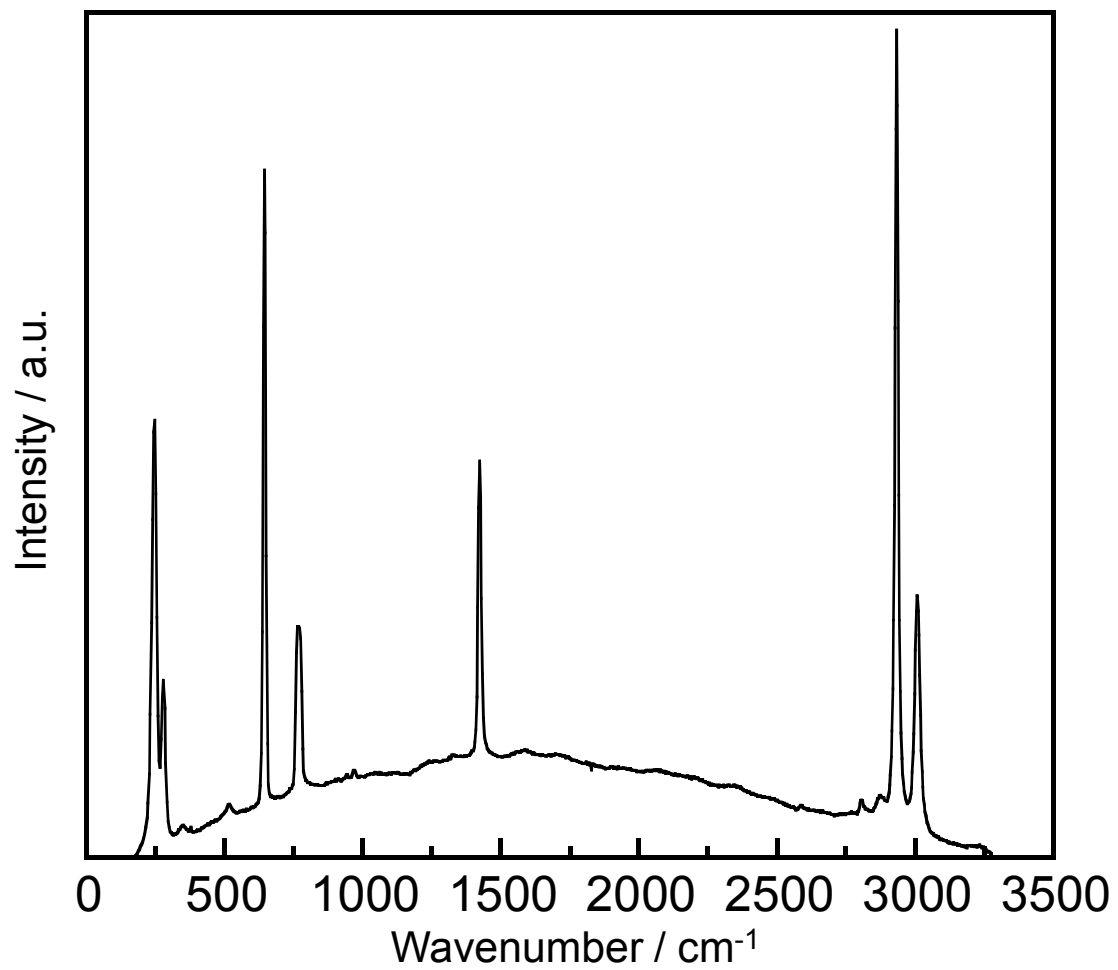
Figure S20 Raman spectrum of [P$_1$][BF$_4$] at 298 K.
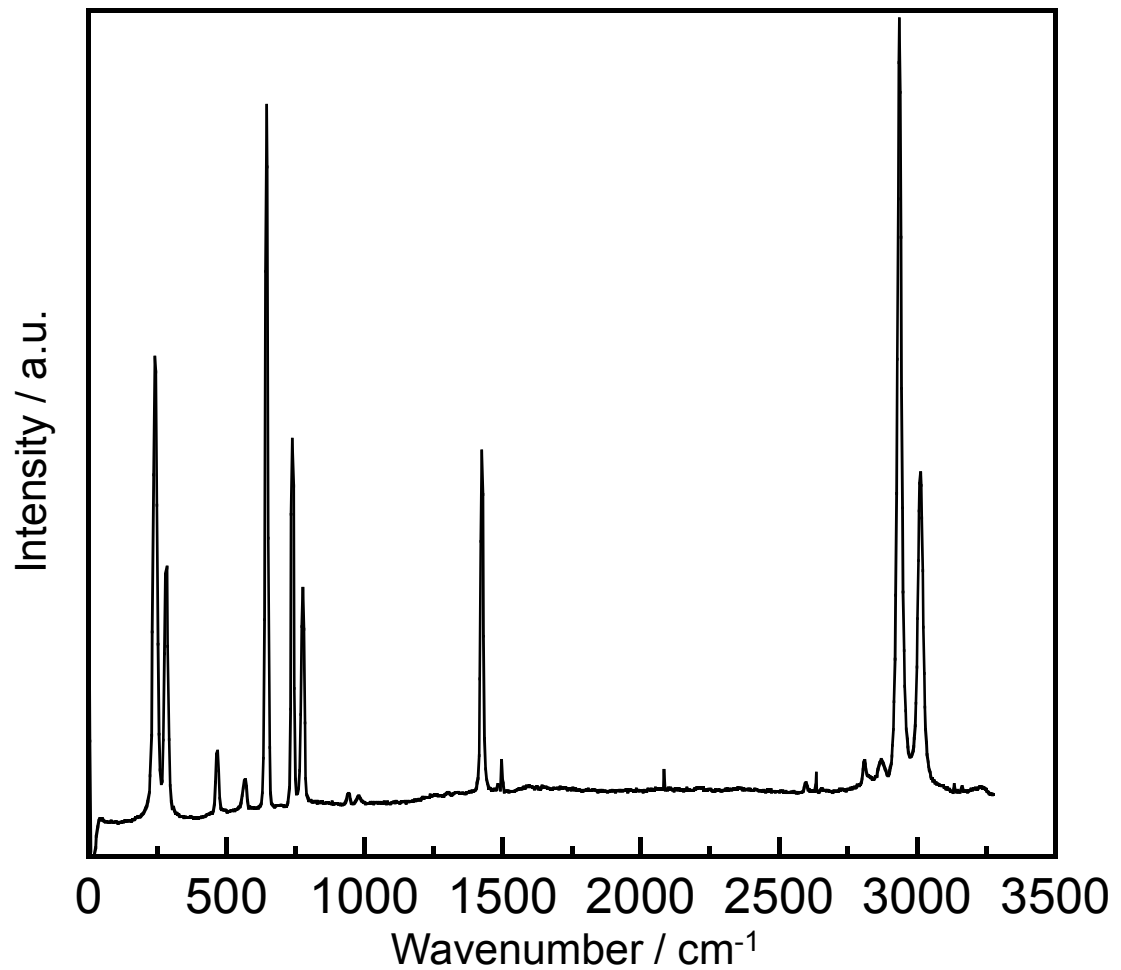
Figure S21 Raman spectrum of [P$_1$][PF$_6$] at 298 K.
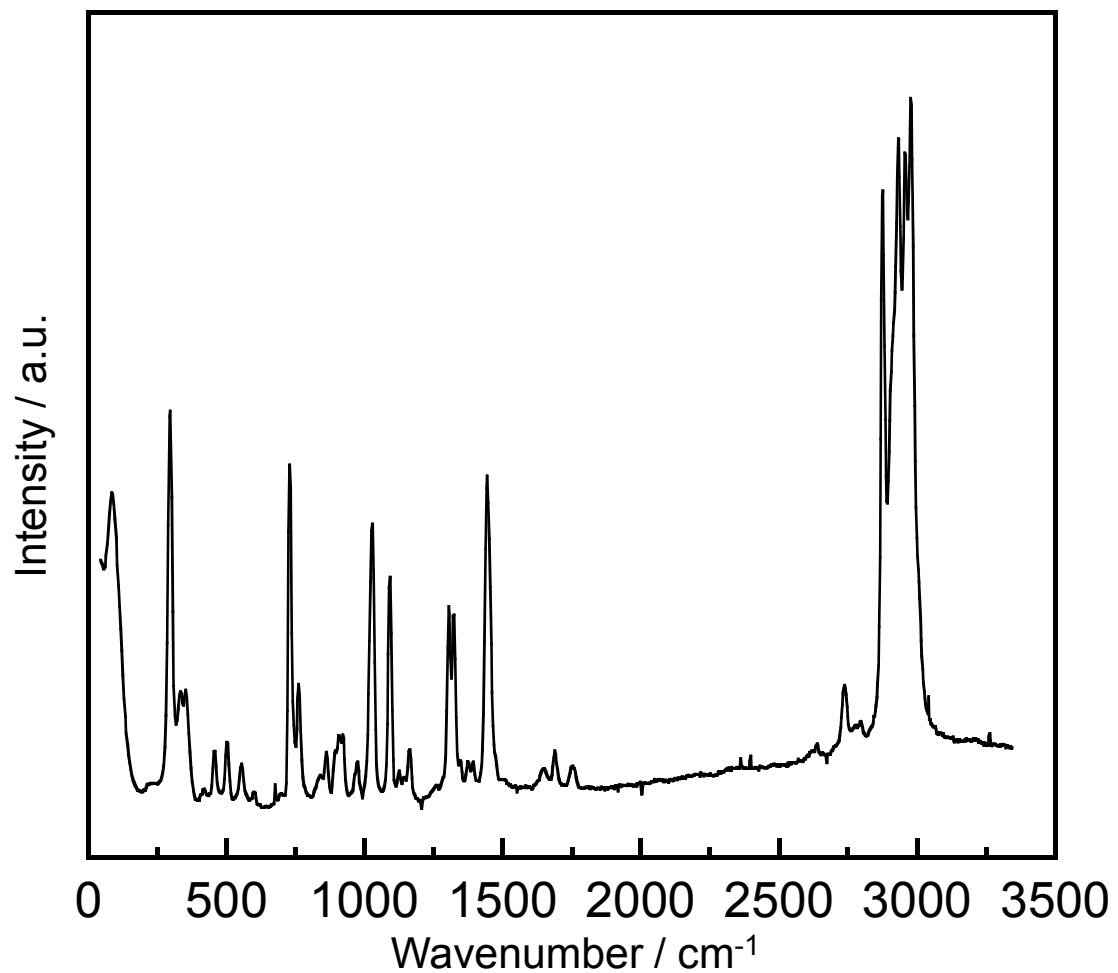
Figure S22 Raman spectrum of $[N_3][PF_6]$ at 298 K.
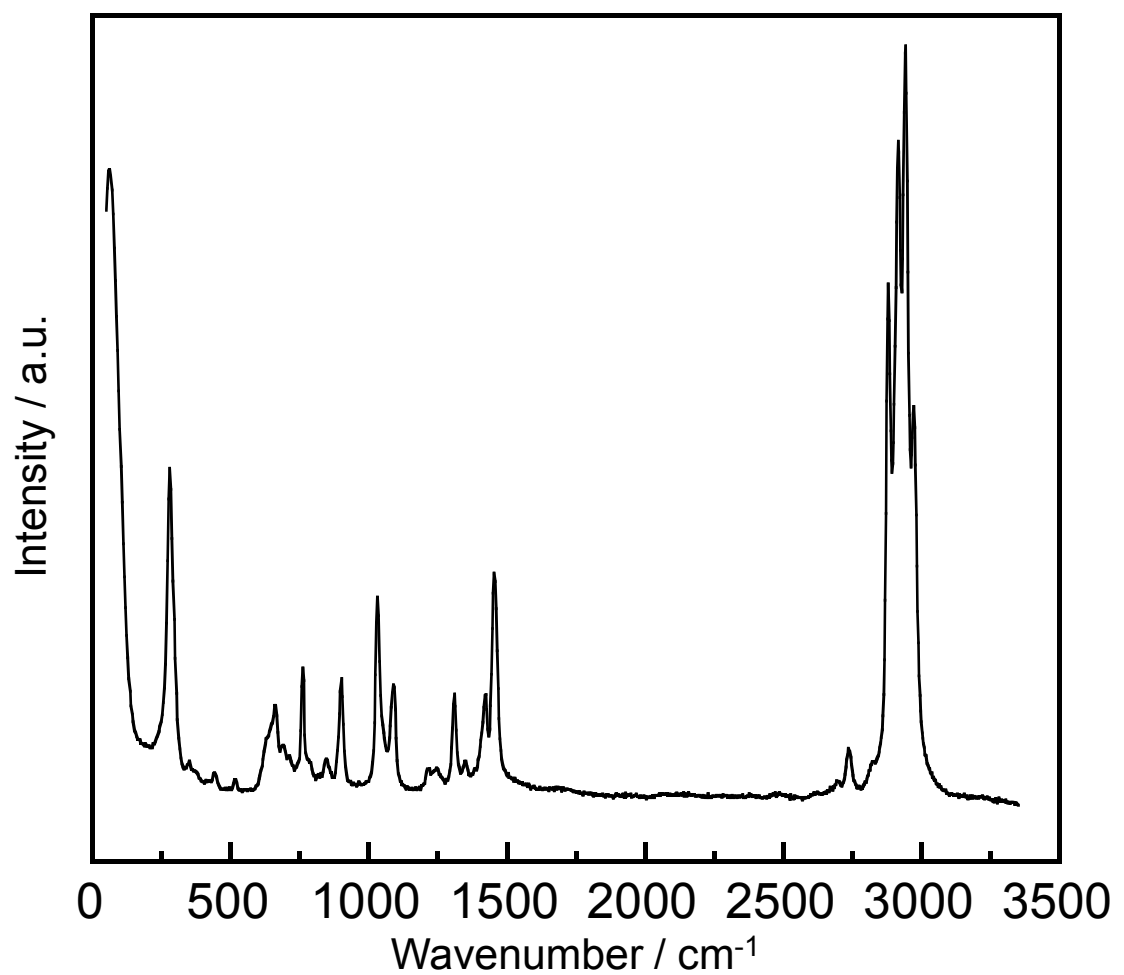
Figure S23 Raman spectrum of [P$_3$][BF$_4$] at 298 K.
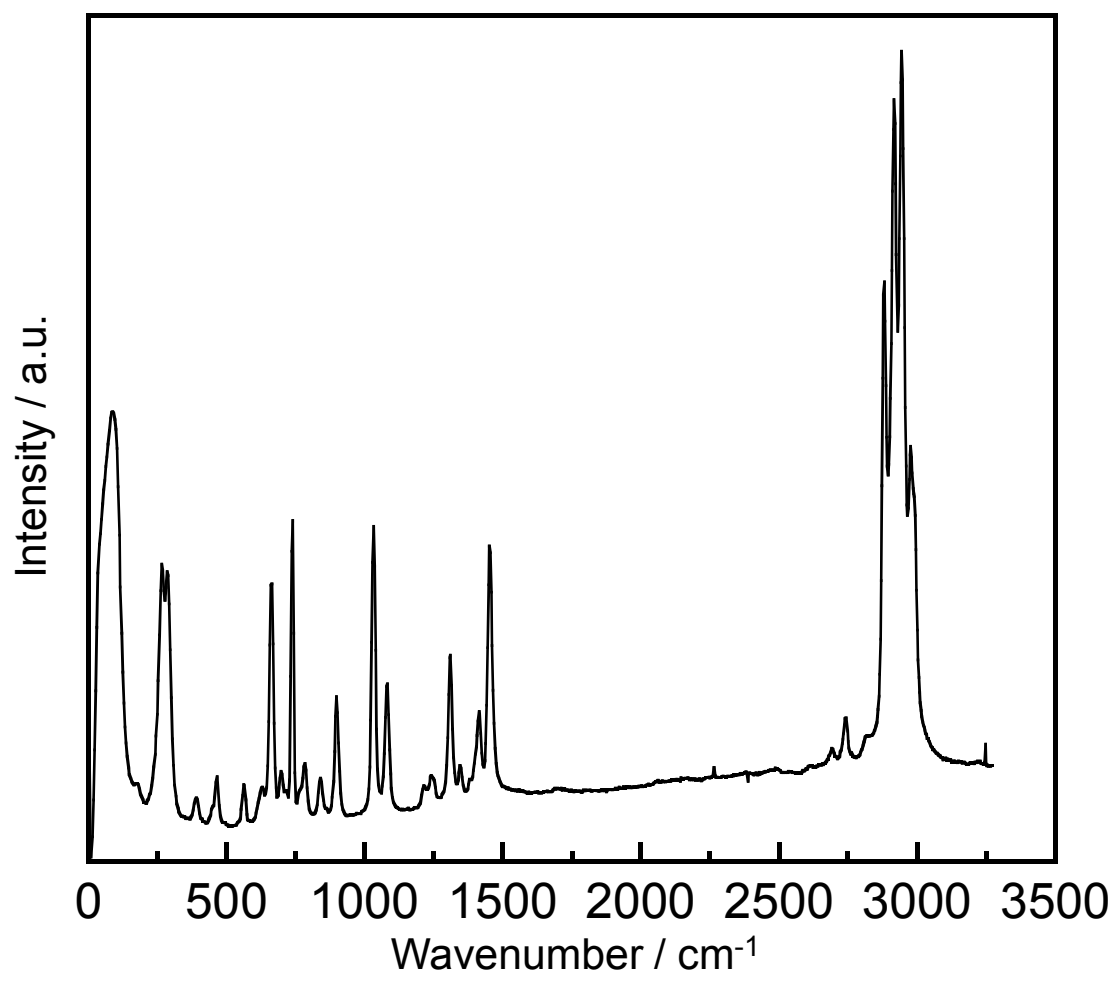
Figure S24 Raman spectrum of [P$_3$][PF$_6$] at 298 K.

2θ
60
50
40
30
20
10

T = 333 K, MoKα
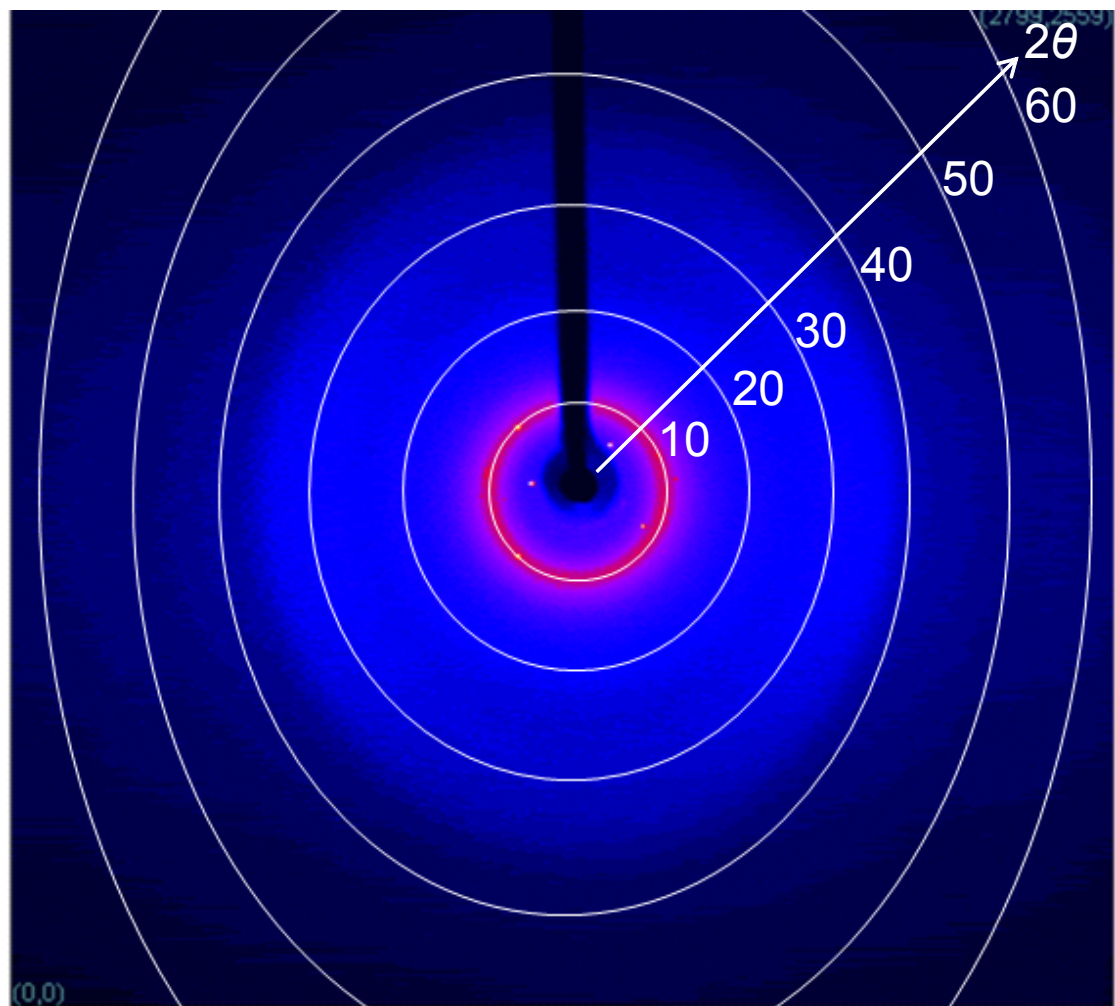
Figure S25 An X-ray diffraction image of Phase I for [P$_4$][PF$_6$] obtained at 333 K.